Heliyon 10 (2024) e38974

Contents lists available at ScienceDirect

Heliyon

journal homepage: www.cell.com/heliyon

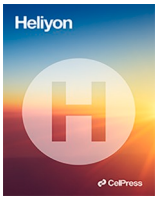

Research article

Hydrate technology for water desalination in the Mekong Delta, Vietnam

Quang Nhat Tran [a,b,1], Nhi Ngoc Thi Vo [a,b,1], Thao Thi Pham [a,b], Hai Son Truong-Lam [a,b,*]

[a] Faculty of Chemistry, University of Science, Ho Chi Minh City, 70000, Viet Nam
[b] Vietnam National University, Ho Chi Minh City, 70000, Viet Nam

ARTICLE INFO

Keywords:
Mekong delta
Saline intrusion
Desalination
Hydrate technology
Hydrate former
Cyclopentane
1,1,1,2-Tetrafluoroethane

ABSTRACT

Freshwater scarcity is a critical issue in Vietnam, particularly in the Mekong Delta, a densely populated region with an agriculture-based economy. This scarcity is largely driven by saltwater intrusion during the dry season, severely affecting both agriculture and the local economy. In response, advanced desalination technologies have been proposed. In this study, we investigated the use of cyclopentane (CP), a liquid guest molecule, and 1,1,1,2-tetrafluoroethane (R134a), a gaseous guest molecule, as hydrate formers to desalinate saline water from the Mekong Delta. This study aimed to evaluate and compare the freshwater recovery efficiencies of these hydrate formers and assess the potential of hydrate technology for practical application in the region. We performed thermodynamic and kinetic investigations on sodium chloride solutions (1.0–3.5 wt %), representing the salinity levels of seawater in the Mekong Delta, to establish a laboratory-scale desalination system. The results showed a consistent thermodynamic trend: the higher concentration of samples leads to the longer time of hydrate formation to achieve the conversion of water into hydrates exceeding 60 %. Additionally, the CP and R134a hydrate structures were characterized using Raman spectroscopy, which revealed significant changes in the water peak and C–H band signal during the hydrate formation process. After a single-stage hydrate treatment using CP and R134a, the removal efficiencies for ions and total dissolved solids in saline water samples from the Mekong Delta exceeded 75 % and 70 %, respectively. These findings serve as a reference for developing a larger-scale hydrate-based desalination technology to address the challenges of saltwater intrusion in the Mekong Delta region.

1. Introduction

Seawater is an abundant and diverse resource that plays crucial roles in various aspects of life and science. Covering most of the Earth's surface, seawater is the largest water source on the planet and the habitat for many marine ecosystems. However, the impacts of climate change, driven by rapid urbanization and industrialization, have led to an increase in natural disasters such as floods, droughts, and saltwater intrusion, which in turn have increased the proportion of seawater relative to freshwater resources. Chemically, seawater contains many dissolved compounds and ions, such as Na^+, Cl^-, Mg^{2+}, Ca^{2+}, and K^+. While these ions are important in

* Corresponding author. Faculty of Chemistry, University of Science, Ho Chi Minh City, 70000, Viet Nam.
E-mail address: tlshai@hcmus.edu.vn (H.S. Truong-Lam).
[1] Quang Nhat Tran and Nhi Ngoc Thi Vo contributed equally to this work.

https://doi.org/10.1016/j.heliyon.2024.e38974
Received 1 July 2024; Received in revised form 3 October 2024; Accepted 3 October 2024
Available online 4 October 2024

various biochemical and industrial processes, they contribute to seawater salinity [1].

The severe scarcity of clean water in many regions worldwide is a major concern, necessitating immediate solutions. Fortunately, clean water can be produced from seawater using desalination technologies. Over time, various methods for treating seawater and converting it into clean water have been researched and developed. Initially, thermal desalination processes were employed, but there has been a gradual shift to membrane technology, representing a significant transition in water treatment technology. Membrane desalination, primarily through reverse osmosis (RO), accounts for around 69 % of the global desalination capacity, and approximately 85 % of the total desalination plants worldwide use membrane-based methods [2]. Other thermal desalination methods, such as multi-stage flash (MSF) distillation and multi-effect distillation (MED), account for approximately 18 % and 7 % of the global desalination capacity, respectively. However, only 2.1 % and 5.6 % of global desalination plants employ MSF and MED, respectively [2]. Additionally, RO, MSF, and MED processes are associated with high energy consumption, complex pretreatment stages, and significant operational costs. These shortcomings have fueled the search for more advanced desalination technologies [3-4.].

Saltwater intrusion, which occurs when saltwater penetrates rivers and canals during high tides, leads to the contamination of freshwater sources. Such intrusion combines saltwater with freshwater, making surface and groundwater unsuitable for drinking or agricultural use [5]. Saltwater intrusion has become increasingly problematic in Vietnam, especially in the Mekong Delta region, where residents are already facing water scarcity. Climate change has been identified as the primary driver of this problem [6]. In Vietnam, saltwater intrusion typically occurs during the dry season, from December to early May, with a peak in late April. In addition to significantly affecting human health, water scarcity related to such intrusions has severe impacts on agriculture. The Mekong Delta region has the largest agricultural output in Vietnam, and one of the worst-affected areas. In 2016, saltwater intrusion extended 20–30 km inland, lasting for 30–40 days and destroying approximately $\sim 2.4 \times 10^5$ ha of rice fields and an estimated economic loss of 445 million USD, or 1.5 % of the total annual rice crop area [7]. This significantly impacted not only Vietnam's agricultural production but also the availability of clean water for local residents.

In this study, we evaluated the salinity conditions in Ben Tre, a province in the Mekong Delta, Vietnam. Ben Tre exhibits a unique geography, bordered by the East Sea and intersected by four major rivers (the Co Chien, Ham Luong, Ba Lai, and Dai Rivers), which makes it particularly vulnerable to saltwater intrusion during the dry season. The coastal districts of Binh Dai, Ba Tri, and Thanh Phu are heavily affected due to their proximity to the sea, whereas inland districts experience lower salinity levels [8]. The Ba Lai River runs through a region characterized by high population density and diverse agricultural activities, encompassing rice cultivation, aquaculture, and fruit orchards [9]. During the dry season, saltwater from the Tien River flows into the Ba Lai River, particularly when the dyke gates are opened. Moreover, this area is adjacent to the East Sea and is generally characterized by low-lying terrain, exacerbating saltwater intrusion [10].

In recent years, RO membrane technology has been the primary method for converting saline water to freshwater in the Mekong Delta. However, RO membranes are prone to clogging by solid residues in saline water, and high salinity levels hinder the filtration process [11]. Additionally, the presence of silt, suspended solids, and hard-to-dissolve compounds in saline water further complicates the treatment process. Therefore, more advanced desalination technologies are needed to address these challenges and improve water treatment.

Hydrate technology, also known as gas hydrate or clathrate hydrate technology, has emerged as a promising alternative. This technology can be used to treat various water types, including seawater, brackish water, and wastewater, and offers significant advantages over RO systems, such as avoiding membrane clogging. For instance, Truong-Lam and colleagues revealed that hydrate technology can be used to treat solutions with salinity levels of up to 15 wt%. They also noted that its potential for treating highly concentrated wastewater that cannot be processed using RO technology [12].

During hydrate formation (crystalline water-based solids physically resembling ice), water molecules create crystalline cages (hydrates) around guest gas or liquid molecules, separating them from the saline solution even at temperatures above the freezing point of water. When these hydrate crystals are melted, they yield freshwater, while the guest molecules can be recycled for further desalination. Studies have shown that when the hydrate cages are fully occupied by guest molecules, the hydrate consists of approximately 85 mol% water and 15 mol% guest molecules [13], demonstrating the significant potential of this method to produce relatively pure water. Compared with to RO, MSF, and MED, hydrate technology requires lower energy consumption, as it operates at temperatures above water's freezing point [14]. Hydrates generally form in three structures: structure I (sI, cubic), structure II (sII, cubic), and structure H (sH, hexagonal), with the type of structure depending on the size of the guest molecules used [15]. For example, sII hydrates, which involve more water molecules per guest molecule, are considered highly effective for desalination [16–19]. Additionally, The solubility of guest molecules also plays a significant role in the quality of water produced during desalination, making the choice of guest molecules critical, as it ensures the low consumption of energy and favors the production of very clean water [20].

Recent research has explored the use of cyclopentane (CP) as a hydrate-forming agent for desalination in NaCl solutions, as reported by Ho-Van et al. [21], as well as applications of gas-phase guest compounds, as detailed by Truong-Lam et al. [20,22]. However, the novelty of this study lies in applying hydrate technology to real-world saline water samples from Ben Tre Province in the Mekong Delta, using both CP and R134a as hydrate formers. These compounds were chosen because they form sII hydrates, which are advantageous for water treatment. CP is particularly attractive because it forms hydrates at atmospheric pressure, simplifying the process and allowing for easy recovery and reuse of CP [23]. Conversely, R134a offers faster kinetics and milder operational conditions [24], but it is also a greenhouse gas, presenting environmental concerns [25].

This study aims to assess the effectiveness of CP and R134a hydrate technologies for desalination of saline water in the Mekong Delta. To date, no comparative studies have examined these two compounds in the context of hydrate-based water treatment. While CP offers a simpler operational mechanism, the rapid kinetics and high-pressure requirements make R134 a complex yet efficient

alternative. This research will provide insights into the suitability of both hydrate formers for large-scale application. Our findings are based on samples from a single province in the Mekong Delta and may not fully represent other regions in Vietnam. Future work could extend the spatial distribution of sampling to evaluate the nationwide applicability of the proposed hydrate technology. While our focus is on desalination of water primarily intended for irrigation, it also addresses the broader issue of freshwater scarcity for agricultural and livestock use. In this way, the study aims to provide a viable solution for applying hydrate technology to desalinate specific real-world water samples.

2. Materials and methods

2.1. Materials

CP with a purity of 96 % was obtained from Aladdin (China), while sodium chloride (NaCl), with a purity of 99.5 %, was sourced from Guangzhou (China). Ethylene glycol was purchased from Xilong (China), and deionized water, with a resistivity of 18 MΩ, was produced in the laboratory. All chemicals used in the experiments were of high purity and were applied as received.

To assess the salinity levels in Ben Tre Province, three sampling locations were chosen, each at varying distances from the sea: Sample A was 15 km inland, Sample B was 5 km inland, and Sample C was 1 km inland (Fig. 1). These locations represent different levels of saltwater intrusion, highlighting the areas most affected by salinity, particularly with regard to agriculture and freshwater scarcity. The sampling procedure adhered to the Vietnamese national standard TCVN 6663–14:2018. After collection, the samples were stored at 4 °C, following TCVN 6663–3:2016 guidelines, until further analysis. The sampling sites were situated along the Ba Lai River, a region bordered by a mangrove forest ecosystem, where saline and seawater samples contain high amounts of sediment and suspended solids. Preliminary processing of the samples was necessary before analysis.

2.2. Apparatus

The desalination process using cyclopentane hydrate (CPH) was conducted using the experimental setup illustrated in Fig. 2. The system comprised a VWR/Polyscience 1140A cooling tank (purchased from Avantor, USA) to maintain thermal stability during hydrate formation, a stirrer with a fixed speed of 300 rpm, and a reaction vessel with a 100 mL capacity. The reaction vessel contained the saline water sample mixed with NaCl solution and cyclopentane. Temperature monitoring was achieved using a thermal sensor, and the collected data were recorded via software. Once the hydrate was formed, it was separated using a low-pressure filter. Any remaining cyclopentane was fully dissociated using a cold centrifuge (Hettich MIKRO 220R, Germany). A salinity measurement machine (86,505 AZ, Taiwan) was used for salinity determination.

2.3. Experimental procedure

Based on the results of the thermal and kinetic analyses, we selected CP as the guest molecule for hydrate formation in this kinetic

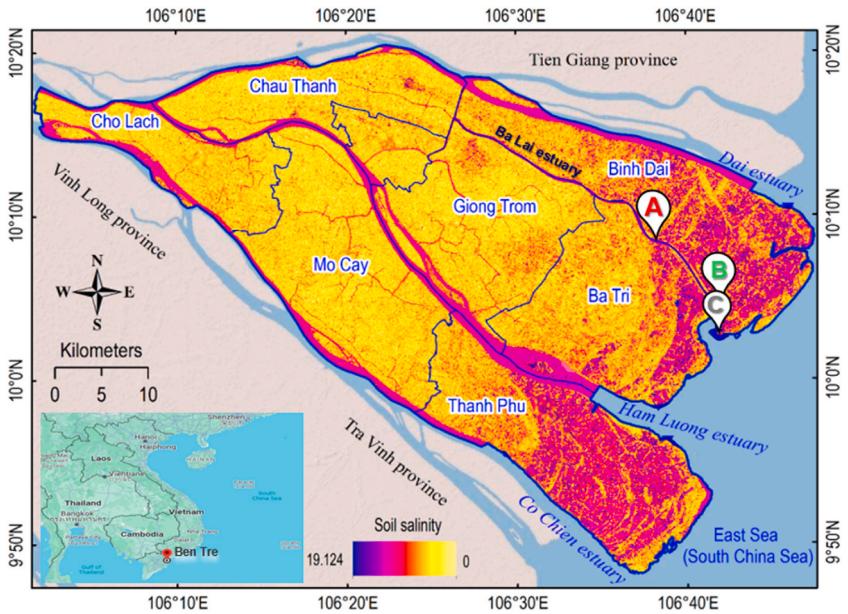

Fig. 1. Salinity distribution map of the Mekong River in Ben Tre province (S‰). Sampling locations (A), (B), and (C) are situated 15, 5, and 1 km inland from the sea, respectively.

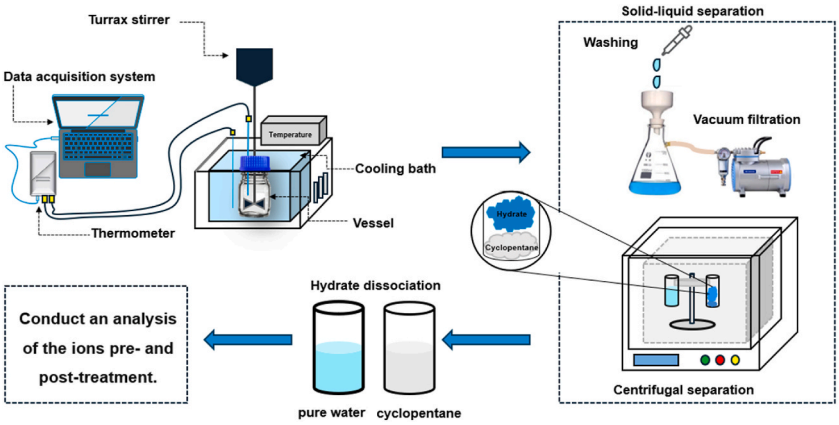

Fig. 2. Schematic of the hydrate-based desalination technique using CPH.

study. Studies have shown that cooling the hydrate to 5.6 K enhances the nucleation process [26,27]. We initiated the reaction between CP and the NaCl solution under fixed conditions in a Duran flask: a CP-to-NaCl solution ratio of 1:3 [27], a reaction temperature of 275.15 K, and a stirring speed of 300 rpm. A 304 stainless steel temperature-controlled refrigeration system equipped with a refrigerated water bath (Haake K15, USA), a temperature sensor, and an exhaust valve was used to maintain stable temperatures throughout the experiment. Ethylene glycol was used as the cooling medium to ensure system stability, maintain temperature throughout the hydrate formation process, and prevent algae growth in the heat bath. Temperature data were monitored and displayed via the thermal control system. The hydrate conversion time, an important focus in this study, was calculated from the onset of hydrate crystal formation. NaCl solutions with varying concentrations (1.0–3.5 wt%) were used for kinetic analysis. A cold centrifuge device set to 268.15 K and 3000 rpm was utilized to separate unreacted saline water from the hydrate crystals, ensuring rapid and accurate sample analysis.

The equilibrium temperature of CPH was measured for Samples A, B, and C, as well as for NaCl solutions of 1, 2, 3.5, and 5 wt%. Hydrate formation occurred in reactors containing 18 mL of a brine and cyclopentane mixture at a molar ratio of 17:1. The reactors were first placed in a freezer at −10 °C overnight, and then immersed in a water-glycol bath at 0 °C. The temperature of the bath was gradually increased in 0.2 °C increments, with each step held for at least 1 h. The equilibrium temperature was recorded as the point at which hydrate crystals were no longer visible with the naked eye.

2.4. Desalination process

The desalination process using CPH was evaluated using saline water samples collected from Ben Tre Province. After a set period of hydrate formation, the CPH crystals were filtered under vacuum to ensure thorough separation from the remaining saltwater. The hydrate crystals were then rinsed with a small amount (1.5 mL) of treated water to remove salt ions adhered to their surfaces, further reducing salinity and improving the efficiency of ion removal. The rinsed hydrates were centrifuged at 3000 rpm for 10 min, facilitating the rapid separation of the CP and water layers upon hydrate dissociation [28]. Finally, clean water was obtained and a certain amount of CP was recovered after the reaction. To efficiently eliminate dissolved CP, the clean water underwent ultrasonic treatment, which recovered around 8%–10 % of the CP in relation to the volume of the desalinated water.

The clean water produced was analyzed for total dissolved solids (TDS) and salinity using a benchtop pH–mV meter (Mettler Toledo, USA). Analytical methods based on Vietnamese national standards (TCVN) were applied to evaluate the concentrations of major ions (Cl^-, SO_4^{2-}, Na^+, K^+, Ca^{2+}, and Mg^{2+}) in both the untreated saline water and the purified water. Cl^- was analyzed using the Mohr titration method, while SO_4^{2-} was analyzed by the SMEWW 4500–SO_4^{2-}.E:2017 turbidimetric method, and Na^+, K^+, Ca^{2+}, and Mg^{2+} were measured using atomic absorption spectrometry (AAS) based on the flame-AAS (F-AAS) technique. Various calculations were performed before and after the treatment, as outlined below.

The mass of water before the hydrate formation process was calculated using Equation (1):

$$m_{w_1} = m_{salt}^{before} - \left(\frac{m_{salt}^{before} \times \left(\frac{S_{salt}^{before}}{10} \right)}{100} \right), \quad (1)$$

where S_{salt}^{before} is the salinity of the initial solution in units of ppt, m_{w_1} and m_{salt}^{before} are the masses of water and salt in the initial saline sample solution, respectively. Similarly, the mass of water after the reaction was calculated using Equation (2):

$$m_{w_2} = m_{salt}^{after} - \left(\frac{m_{salt}^{after} \times \left(\frac{S_{salt}^{after}}{10} \right)}{100} \right), \quad (2)$$

where m_{w_2} and m_{salt}^{before} are the masses of freshwater and salt produced from the dissociated hydrate, respectively, and S_{salt}^{before} is the salinity of the dissociated solution. The percentage of water converted into hydrate (H_w) was calculated as:

$$H_w = \frac{m_{w_1} - m_{w_2}}{m_{w_1}} \times 100\%. \quad (3)$$

Furthermore, the desalination efficiency was evaluated for each sample using Equation (4):

$$H_{removal\ efficiency} = \frac{C_{salt}^{0} - C_{salt}^{hydrate}}{C_{salt}^{0}} \times 100\%, \quad (4)$$

where C_{salt}^{0} is the initial salt concentration of the saline water and $C_{salt}^{hydrate}$ is the salt concentration of water produced from the dissociated CPH.

3. Results & discussion

3.1. Thermodynamic and kinetic behaviors of cyclopentane hydrate and 1,1,1,2-tetrafluoroethane hydrate

The results demonstrated that high desalination efficiency using CPH could be achieved by optimizing the conditions of the system. Therefore, we focused on studying the kinetic and thermodynamic behaviors of CPH in NaCl solutions (to represent saline environment). This approach aimed to refine the desalination process for practical application in saline water treatment and freshwater recovery. Phase equilibrium plays a crucial role in the hydrate formation process and influences the thermodynamic behavior during kinetic studies [29]. We used the isochoric method to determine the phase equilibrium of CPH in NaCl solutions, as described in our previous studies [12,34]. Fig. 3 illustrates the equilibrium temperature of CPH in NaCl solutions of varying concentrations of 1.0, 2.0, 3.5, and 5.0 wt%. The results indicate a correlation between higher salt concentrations and lower equilibrium temperatures for hydrate dissociation, which aligns with the findings of Ho-Van et al. [30]. The equilibrium temperatures observed in this study are also consistent with those obtained by Mok et al. and Mallek et al. [29,31,32]. This phase equilibrium data provided the foundation for selecting appropriate operating conditions for the CPH-based desalination system.

To evaluate the dynamic behavior of CPH, we conducted laboratory-scale experiments using NaCl solutions as a representative model for saline water [33]. Na^+ and Cl^- ions account for the majority of the ionic content in saline and seawater, making NaCl solutions a suitable proxy [9]. In the Mekong Delta, water with a salinity above 0.5 wt% is considered saline, with levels typically lower than seawater. Therefore, NaCl concentrations ranging from 1.0 to 3.5 wt% were selected for the experiments, as described in Section 2.2. Fig. 4 shows the conversion efficiency of water into hydrates over time for different NaCl concentrations. The colored dots represent the conversion efficiencies for NaCl solutions of 1.0–3.5 wt%, with colors ranging from red, orange, and yellow to light blue, dark blue, and gray. During our experiments, we observed that the conversion rate decreases as the NaCl concentration increases. This behavior can be attributed to the excess salt content, which inhibits hydrate nucleation by preventing the formation of hydrate

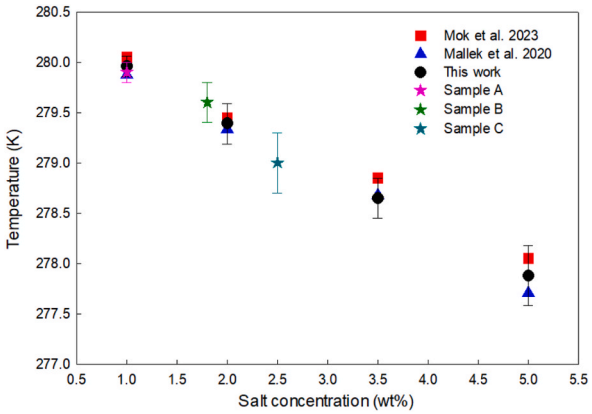

Fig. 3. Equilibrium-dissociation temperatures of CPH in NaCl solutions of various concentrations. The black circles indicate the equilibrium temperatures of CPH at several NaCl concentrations. The pink, green, and dark green symbols show the equilibrium temperatures of CPH for Samples A, B, and C, respectively. The results are compared with those obtained by Mok et al. [29] (red squares) and Mallek et al. [31] (blue triangles).

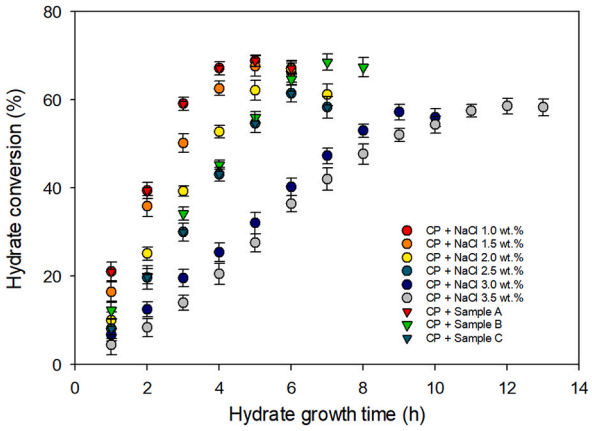

Fig. 4. Conversion of water into hydrates using saline water and NaCl solutions with varying concentrations over time. The red, orange, yellow, green, blue, and gray dots represent the conversion efficiencies of water into hydrate for NaCl solutions at different concentrations (1.0–3.5 wt%). The red, green, and dark green triangle dots represent the conversion efficiency of water into hydrate for Sample A, Sample B, and Sample C, respectively. The error bars indicate standard deviations.

structures [34]. Moreover, as crystal formation progresses, the driving-force temperature required for crystal growth decreases due to the phase equilibrium shift caused by the increasing salinity in the residual solution.

Fig. 4 also indicates that around 60 % of the water is converted into hydrate early in the process, with the rate of conversion slowing down as the reaction time increases. This observation formed the basis for opting to perform this study in a saline water background. Additionally, the green triangular shape in Fig. 4 represents a saline water sample with a salinity of ~1.8 wt%. This finding indicated some similarities in the hydrate formation process, with conversions typically ranging between 2.0 and 2.5 wt%. Based on this, we concluded that the hydrate formation of the 1.8 wt% background sample may cease after approximately 6 h, as only minor changes in hydrate conversion are observed between 6 and 7 h. This finding emphasizes the importance of reaction time optimization for industrial applications, where shorter reaction times translate into increased cost efficiency. Therefore, we recommend that future CPH studies should be based on this thermodynamic and kinetic survey chart.

Research by Truong-Lam et al. [12] into the thermodynamics of gaseous guest molecules suggest that R134a is a promising candidate for hydrate-based desalination [20]. However, most studies have focused on the application of R134a to seawater desalination rather than saline water. In this study, we applied R134a to saline water samples from the Mekong Delta using the apparatus developed by Truong-Lam et al. to compare both hydrate-forming substances (CPH and R134a) and expand the research scope.

Thermodynamic studies were conducted both experimentally and using the Hu-Lee-Sum (HLS) correlation methods. As shown in Fig. 5, the hydrate formation conditions for saline water fall between those of pure water and 3.5 wt% NaCl solutions. The experimental and theoretical curves display only minor differences. These results revealed a similar trend in both R134a and CP: as the salt concentration increases, the conditions for hydrate formation become more restricted, particularly under conditions of low

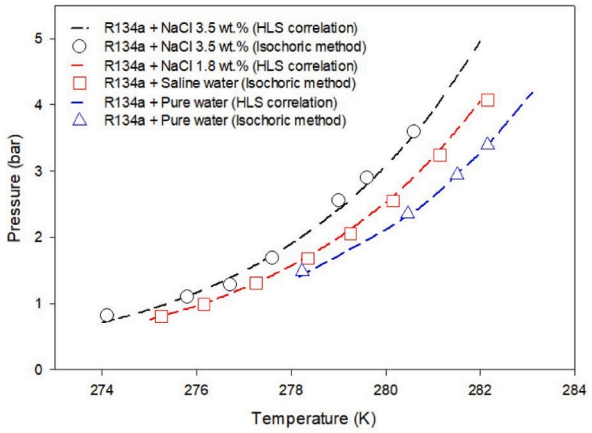

Fig. 5. R134a hydrate equilibrium phase in NaCl solutions (3.5 and 1.8 wt%) and pure water. The phase equilibria of R134a in saline water (this study) were compared with those in 3.5 wt% NaCl solutions and pure water (from previous studies) based on reported experimental values. The symbols and dashed lines represent results obtained by the isochoric and HLS correlation methods, respectively. The black, red, and blue colors correspond to 3.5 wt% NaCl, 1.8 wt% NaCl, and pure water, respectively.

temperature and high pressure.

3.2. Raman spectroscopy of the cyclopentane hydrate and R134a hydrate

Raman spectroscopy was used to monitor the hydrate formation processes of CP and R134a to ensure that the results were not influenced by external factors. Fig. 6 displays the vibrational regions before and after hydrate formation. To better understand the formation process, we performed Raman measurements across three regions: saline water without CP, saline water with CP, and hydrate crystals after 2 h of development (Fig. 6), with a focus on the 2800–3000 cm^{-1} region, corresponding to the C–H band. The CP hydrate exhibited Raman peaks at 2881 and 2955 cm^{-1}. The positions of these peaks did not shift significantly compared to those of liquid CP, indicating no significant difference in the vibrational and rotational motions of CP molecules between the hydrate and liquid state. Before hydrate formation in saline water, only water peaks were observed, with no CPH signal. Following the onset of hydrate formation, peaks corresponding to water decreased, and those of CPH became more pronounced. Once full crystal formation was achieved, the C–H bands of CP were detected with lower intensity due to the low concentration of solid crystals, confirming that hydrate formation had taken place. These results align with the findings of Lee et al. [17].

Next, we studied the kinetics of R134a hydrate formation using Raman spectroscopy (Fig. 7). Raman peaks were detected at 835, and 2988 cm^{-1}, which represent C–C and C–H bands, respectively, in dissolved R134a. Raman peaks at around 836, and 2979 cm^{-1} correspond to the large cages occupied by R134a. While only minor wavelength differences occurred in the C–C band region, a significant shift in the peak position of the C–H band between the dissolved R134a and R134a hydrates confirmed hydrate formation. The structure II (sII) of the R134a hydrate in the saline water sample remained unchanged, as evidenced by the lack of variation in the peak positions at 836, and 2979 cm^{-1} during hydrate formation The results indicate that R134a molecules were enclathrated into the large cages ($5^{1,2}6^4$) of the structure II-unit lattice, with no detectable bands corresponding to the occupation of smaller cages (5^{12}). These results are consistent with the previous findings of Truong-Lam et al. [12], [20], [35].

3.3. Evaluation of the desalination process

As seen in several previous studies, R134a has been widely explored across various sample matrices. In this study, we used R134a as a benchmark for comparison with CPH based on the results from NaCl solution tests at different concentrations, which were largely consistent with those of CPH. However, for the desalination of saline water samples from Ben Tre, CPH was chosen due to its simpler operational mechanism and to mitigate the environmental impact associated with R134a.

To further improve desalination efficiency, particularly in the removal of salt ions from the surface of hydrate crystals, a rinsing method was integrated into the separation process. As shown in Fig. 8, two types of rinse water—deionized water and saline sample solution—were assessed based on their rinse volumes. The results demonstrated a significant improvement in desalination efficiency with increased rinse volumes. Without rinsing, the efficiency was around 45 %, but this increased to approximately 75 % when 3 mL of rinse water was used. The increased rinse volume effectively removed surface ions from the hydrate crystals, improving overall desalination performance. However, larger rinse volumes also led to increased dissociation of the hydrates during the rinsing process, reducing the amount of recovered clean water. The data also revealed that desalination efficiency exceeded 70 % without further improvement when the rinse volume exceeded 1.5 mL. To balance desalination efficiency with clean water recovery while minimizing

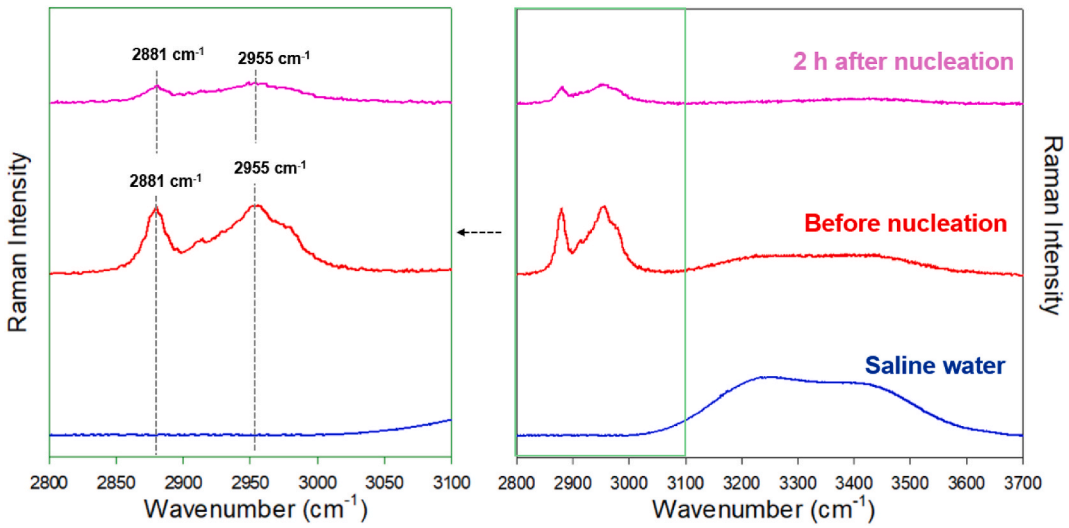

Fig. 6. Raman spectra of saline water samples and cyclopentane in the C–H band region (2800–3000 cm^{-1}), corresponding to the hydrate nucleation process. Raman spectroscopy was performed in three regions: (i) saline water without cyclopentane (blue line), (ii) saline water stirred with cyclopentane (red line), and (iii) cyclopentane hydrate after nucleation for 2 h.

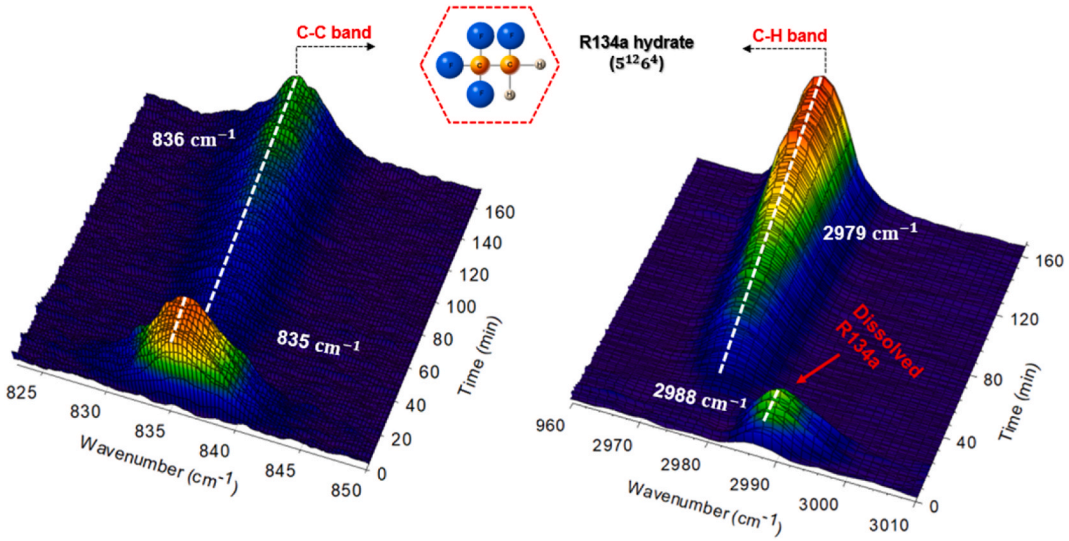

Fig. 7. In-situ Raman spectroscopy monitoring the formation of R134a hydrate in a saline water sample (Sample B, 1.8 wt%) at 0.20 MPa and 274.15 K. The spectra represent the C–C and C–H bands of R134a during hydrate formation.

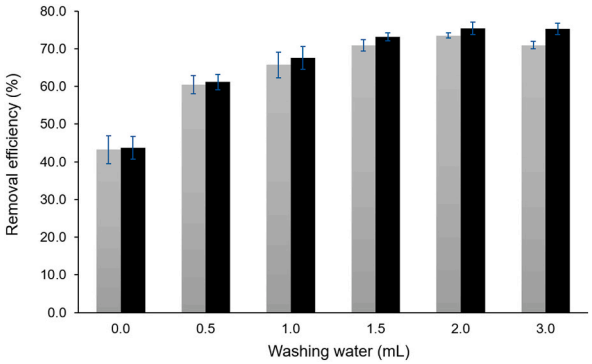

Fig. 8. Effect of rinse water volume on salt removal after hydrate formation. The gray and black columns represent rinsing using saline sample solution and deionized water, respectively. The error bars indicate standard deviations.

the use of deionized water, which is crucial given current freshwater shortages [36], 1.5 mL was selected as the optimal rinse volume, representing approximately 10 % of the sample volume. The data in Fig. 8 revealed no significant difference in desalination efficiency between deionized water and saline sample solution within the margin of error. This suggests that the saline sample solution can be an effective alternative to deionized water for rinsing, addressing concerns about excessive pure water consumption.

As illustrated in Fig. 9 and Table 1, a single stage of CPH treatment successfully removed over 70 % of ions from saline water samples collected from the Mekong Delta. Specifically, ion-removal efficiency ranged between 74.1 % and 82.8 %, while TDS removal efficiency ranged from 70.3 % to 72.9 %. These results highlight the effectiveness of CPH technology for desalinating saline water in regions affected by saltwater intrusion. Furthermore, the technology demonstrated consistent desalination performance across samples with varying salt concentrations, suggesting that CPH is highly effective in removing major ions from a wide range of saline water samples, particularly in salt-impacted areas like Ben Tre Province. Furthermore, these findings are consistent with our previous research on gas hydrate technology for seawater desalination. Table 1 also shows that salinity decreases as sampling locations move further inland, indicating lower concentrations of dissolved ions. Despite this, the ion concentration profiles remained uniform across locations, with no significant variation in the relative concentrations of individual ions. This uniformity is due to the fact that saline water is essentially diluted seawater, meaning that changes in salinity affect the TDS without altering the relative proportions of ions. This observation is consistent with our earlier findings regarding the characteristics of saline water [12].

4. Conclusions

In this study, we evaluated and compared two hydrate-forming compounds, CP and R134a, for their effectiveness in desalinating saline water samples collected from Ben Tre Province in the Mekong Delta, Vietnam. Our thermodynamic analysis of both hydrate

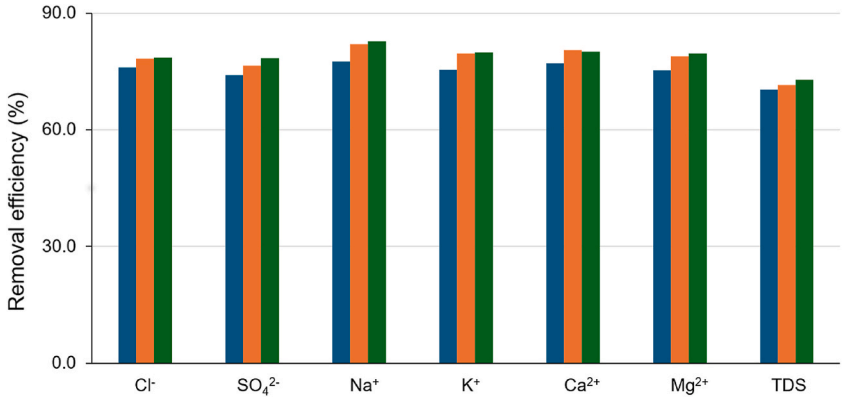

Fig. 9. Results of saline water desalination tests using CPH. The blue, orange, and green columns represent the ion-removal efficiencies of the technology for saline water with concentrations of 1.0, 1.8, and 2.5 wt%, respectively.

Table 1
Experimental salt concentrations and their removal efficiencies using CPH.

Test		Ion concentration (mg/L)[a]						TDS (ppm)[b]
		Cl^-	SO_4^{2-}	Na^+	K^+	Ca^{2+}	Mg^{2+}	
Saline water (C_0)	A[c]	6169 ± 35	678 ± 7	2981 ± 40	169 ± 1	156 ± 2	400 ± 2	7400 ± 0.1
	B[c]	11,203 ± 71	1268 ±12	5328 ± 36	298 ± 1	232 ± 1	632 ± 4	12,400 ± 0.1
	C[c]	16,131 ± 87	1894 ± 17	7612 ± 114	458 ± 2	382 ± 2	1133 ± 1	15,500 ± 0.6
Residual water (C_H)	A[d]	1475 ± 8	176 ± 2	670 ± 9	41.4 ± 0.1	35.7 ± 0.1	98.6 ± 0.6	2200 ± 0.2
	B[d]	2435 ± 13	297 ± 3	950 ± 11	60.7 ± 0.3	45.1 ± 0.2	133 ± 1	2900 ± 0.2
	C[d]	3446 ± 19	407 ± 4	1919 ± 23	92.2 ± 0.4	76 ± 1	230.3 ± 1.8	5200 ± 0.2
Removal efficiency (%)[e]	A	76.1	74.1	77.5	75.5	77.1	75.4	70.3
	B	78.3	76.6	82.1	79.6	80.6	78.9	71.5
	C	78.6	78.5	82.8	79.9	80.1	79.7	72.9

[a] Each cation and anion was analyzed by F-AAS, Mohr's method, and the turbidimetric method.
[b] Total TDS analyzed using a conductivity meter.
[c] Initial concentration of the feed water.
[d] Final concentration of the residual water in the reactor measured 4 h (A), 6 h (B), and 7 h (C) after nucleation.
[e] $\%\text{Removal efficiency} = \frac{C^0_{salt} - C^{hydrate}_{salt}}{C^0_{salt}} \times 100.$

formers demonstrated improvements in the efficiency of the desalination process using hydrate technology. By examining the amount of water converted into hydrate at various salt concentrations using CPH, we were able to effectively control the hydrate formation process, simplifying the monitoring and optimization of saline water desalination. While R134a, a gaseous hydrate former, has potential for desalination, we chose not to apply it to the saline water samples from the Mekong Delta due to its environmental impact as a greenhouse gas and the complexity of operating the necessary equipment. Based on the salt-removal efficiency of the CPH-based hydrate technology (>75 %), as well as favorable operational conditions and operating equipment requirements, we recommended it as a more suitable saline water desalination method for the Mekong Delta. These findings provide a foundation for developing larger-scale hydrate-based desalination technologies to address the issue of saltwater intrusion in the Mekong Delta region.

Data availability statement

No data was used for the research described in the article.

CRediT authorship contribution statement

Quang Nhat Tran: Writing – review & editing, Writing – original draft, Validation, Methodology, Investigation, Formal analysis. **Nhi Ngoc Thi Vo:** Writing – review & editing, Writing – original draft, Validation, Methodology, Investigation, Formal analysis. **Hai Son Truong-Lam:** Writing – review & editing, Writing – original draft, Validation, Supervision, Methodology, Conceptualization, Validation, Methodology, Investigation, Formal analysis.

Declaration of competing interest

The authors declare that they have no known competing financial interests or personal relationships that could have appeared to influence the work reported in this paper.

Acknowledgment

This research is funded by Vietnam National University Ho Chi Minh City (VNUHCM) under grant number B2023-18-05, to Truong-Lam Son Hai. The authors express their gratitude to Dr. Ju Dong Lee, Korea Institute of Industrial Technology for their generous support in providing the Raman Spectrometer, and hydrate apparatus equipment necessary for conducting the experiments.

Appendix A. Supplementary data

Supplementary data to this article can be found online at https://doi.org/10.1016/j.heliyon.2024.e38974.

References

[1] B.A. Sharkh, A.A. Al-Amoudi, M. Farooque, C.M. Fellows, S. Ihm, S. Lee, S. Li, N. Voutchkov, Seawater desalination concentrate—a new frontier for sustainable mining of valuable minerals, Npj Clean Water 5 (2022) 1–16, https://doi.org/10.1038/s41545-022-00153-6.
[2] K. Elsaid, M. Kamil, E.T. Sayed, M.A. Abdelkareem, T. Wilberforce, A. Olabi, Environmental impact of desalination technologies: a review, Sci. Total Environ. 748 (2020) 141528, https://doi.org/10.1016/j.scitotenv.2020.141528.
[3] F.E. Ahmed, A. Khalil, N. Hilal, Emerging desalination technologies: current status, challenges and future trends, Desalination 517 (2021) 115183, https://doi.org/10.1016/j.desal.2021.115183.
[4] A. Saavedra, H. Valdés, A. Mahn, O. Acosta, Comparative analysis of conventional and emerging technologies for seawater desalination: northern Chile as a case study, Membranes 11 (2021), https://doi.org/10.3390/membranes11030180.
[5] B. Liu, S. Peng, Y. Liao, H. Wang, The characteristics and causes of increasingly severe saltwater intrusion in Pearl River Estuary, Estuar. Coast Shelf Sci. 220 (2019) 54–63, https://doi.org/10.1016/j.ecss.2019.02.041.
[6] F.G. Renaud, T.T.H. Le, C. Lindener, V.T. Guong, Z. Sebesvari, Resilience and shifts in agro-ecosystems facing increasing sea-level rise and salinity intrusion in Ben Tre Province, Mekong Delta, Clim. Change 133 (2015) 69–84, https://doi.org/10.1007/s10584-014-1113-4.
[7] H.H. Loc, M. Low Lixian, E. Park, T.D. Dung, S. Shrestha, Y.J. Yoon, How the saline water intrusion has reshaped the agricultural landscape of the Vietnamese Mekong Delta, a review, Sci. Total Environ. 794 (2021) 148651, https://doi.org/10.1016/j.scitotenv.2021.148651.
[8] P.V. Hoa, N.V. Giang, N.A. Binh, L.V.H. Hai, T.D. Pham, M. Hasanlou, D.T. Bui, Soil salinity mapping using SAR Sentinel-1 data and advanced machine learning algorithms: a case study at Ben Tre Province of the Mekong River Delta (Vietnam), Rem. Sens. 11 (2019) 1–21, https://doi.org/10.3390/rs11020128.
[9] N.T. Nam, P.T.B. Thuc, D.A. Dao, N.D. Thien, N.H. Au, D.D. Tran, Assessing climate-driven salinity intrusion through water accounting: a case study in ben Tre province for more sustainable water management plans, Sustainability 15 (2023) 9110, https://doi.org/10.3390/su15119110.
[10] B.K. Veettil, N.X. Quang, N.T. Thu Trang, Changes in mangrove vegetation, aquaculture and paddy cultivation in the Mekong Delta: a study from Ben Tre Province, southern Vietnam, Estuar. Coast Shelf Sci. 226 (2019) 106273, https://doi.org/10.1016/j.ecss.2019.106273.
[11] S.F. Anis, R. Hashaikeh, N. Hilal, Reverse osmosis pretreatment technologies and future trends: a comprehensive review, Desalination 452 (2019) 159–195, https://doi.org/10.1016/j.desal.2018.11.006.D.C.Url. Reverse Osmosis Pretreatment Technologies and Future Trends : a, (2019).
[12] H.S. Truong-Lam, S.D. Seo, C. Jeon, G. pio Lee, J.D. Lee, A gas hydrate process for high-salinity water and wastewater purification, Desalination 529 (2022) 115651, https://doi.org/10.1016/j.desal.2022.115651.
[13] E.D. Sloan, Fundamental principles and applications of natural gas hydrates, Nature 426 (2003) 353–359, https://doi.org/10.1038/nature02135.
[14] P. Babu, A. Nambiar, T. He, I.A. Karimi, J.D. Lee, P. Englezos, P. Linga, A review of clathrate hydrate based desalination to strengthen energy–water nexus, ACS Sustain. Chem. Eng. 6 (2018) 8093–8107, https://doi.org/10.1021/acssuschemeng.8b01616.
[15] M. Khurana, Z. Yin, P. Linga, A review of clathrate hydrate nucleation, ACS Sustain. Chem. Eng. 5 (2017) 11176–11203, https://doi.org/10.1021/acssuschemeng.7b03238.
[16] H.S. Truong-Lam, D. Van Le, T.P. Nguyen, M.T.T. Nguyen, Simulated and experimental thermodynamic investigations for the selection of suitable hydrate formers for water treatment, Vietnam J. Chem. 61 (2023) 33–37, https://doi.org/10.1002/vjch.202300050.
[17] J. Lee, Y.K. Jin, Y. Seo, Characterization of cyclopentane clathrates with gaseous guests for gas storage and separation, Chem. Eng. J. 338 (2018) 572–578, https://doi.org/10.1016/j.cej.2018.01.054.
[18] R. Du, Y. Fu, L. Zhang, J. Zhao, Y. Song, Z. Ling, Desalination of high-salt brine via carbon materials promoted cyclopentane hydrate formation, Desalination 534 (2022) 115785, https://doi.org/10.1016/j.desal.2022.115785.
[19] H.S. Truong-Lam, S.D. Seo, C. Jeon, J.D. Lee, Dynamic analysis of growth of ice and hydrate crystals by in situ Raman and their significance in freezing desalination, Cryst. Growth Des. 21 (2021) 6512–6522, https://doi.org/10.1021/acs.cgd.1c00952.
[20] H.S. Truong-Lam, S. Lee, C. Jeon, S. Seo, K.C. Kang, J.D. Lee, Effects of salinity on hydrate phase equilibrium and kinetics of SF6, HFC134a, and their mixture, J. Chem. Eng. Data 66 (2021) 2295–2302, https://doi.org/10.1021/acs.jced.1c00139.
[21] S. Ho-Van, B. Bouillot, J. Douzet, S.M. Babakhani, J.M. Herri, Cyclopentane hydrates-A candidate for desalination? J. Environ. Chem. Eng. 7 (2019) 103359 https://doi.org/10.1016/j.jece.2019.103359.
[22] S.D. Seo, H.S. Truong-Lam, C. Jeon, J. Han, K.C. Kang, S. Lee, J.D. Lee, Simultaneous removal of multi-nuclide (Sr2+, Co2+, Cs+, and I-) from aquatic environments using a hydrate-based water purification process, J. Hazard Mater. 462 (2024) 132700, https://doi.org/10.1016/j.jhazmat.2023.132700.
[23] E. Brown, M.N. Khan, D. Salmin, J. Wells, S. Wang, C.J. Peters, C.A. Koh, Cyclopentane hydrate cohesion measurements and phase equilibrium predictions, J. Nat. Gas Sci. Eng. 35 (2016) 1435–1440, https://doi.org/10.1016/j.jngse.2016.05.016.
[24] S.D. Seo, S.Y. Hong, A.K. Sum, K.H. Lee, J.D. Lee, B.R. Lee, Thermodynamic and kinetic analysis of gas hydrates for desalination of saturated salinity water, Chem. Eng. J. 370 (2019) 980–987, https://doi.org/10.1016/j.cej.2019.03.278.
[25] D.I.A. McKay, A. Staal, J.F. Abrams, R. Winkelmann, B. Sakschewski, S. Loriani, I. Fetzer, S.E. Cornell, J. Rockström, T.M. Lenton, Exceeding 1.5°C global warming could trigger multiple climate tipping points, Science (2022) 377, https://doi.org/10.1126/science.abn7950.
[26] D. Corak, T. Barth, S. Høiland, T. Skodvin, R. Larsen, T. Skjetne, Effect of subcooling and amount of hydrate former on formation of cyclopentane hydrates in brine, Desalination 278 (2011) 268–274, https://doi.org/10.1016/j.desal.2011.05.035.
[27] S. Han, J.Y. Shin, Y.W. Rhee, S.P. Kang, Enhanced efficiency of salt removal from brine for cyclopentane hydrates by washing, centrifuging, and sweating, Desalination 354 (2014) 17–22, https://doi.org/10.1016/j.desal.2014.09.023.

[28] H. Xu, M.N. Khan, C.J. Peters, E.D. Sloan, C.A. Koh, Hydrate-based desalination using cyclopentane hydrates at atmospheric pressure, J. Chem. Eng. Data 63 (2018) 1081–1087, https://doi.org/10.1021/acs.jced.7b00815.
[29] J. Mok, M. Park, W. Choi, K.C. Kang, S. Lee, J.D. Lee, Y. Seo, Investigation of theoretical maximum water yield and efficiency-optimized temperature for cyclopentane hydrate-based desalination, Water Res. 246 (2023) 120707, https://doi.org/10.1016/j.watres.2023.120707.
[30] S. Ho-Van, B. Bouillot, D. Garcia, J. Douzet, A. Cameirao, S. Maghsoodloo-Babakhani, J.M. Herri, Crystallization mechanisms and rates of cyclopentane hydrates formation in brine, Chem. Eng. Technol. 42 (2019) 1481–1491, https://doi.org/10.1002/ceat.201800746.
[31] R. Mallek, C. Miqueu, M. Jacob, P. Le Mélinaire, C. Dicharry, Effect of porous activated carbon particles soaked in cyclopentane on CP-hydrate formation in synthetic produced water, J. Water Process Eng. 38 (2020), https://doi.org/10.1016/j.jwpe.2020.101660.
[32] Z. Qiao, Z. Wang, C. Zhang, S. Yuan, Y. Zhu, J. Wang, PVAm–PIP/PS composite membrane with high performance for CO_2/N_2 separation, AIChE J. 59 (2012) 215–228, https://doi.org/10.1002/aic.
[33] H.P. Veluswamy, P. Linga, Natural gas hydrate formation using saline/seawater for gas storage application, Energy Fuel. 35 (2021) 5988–6002, https://doi.org/10.1021/acs.energyfuels.1c00399.
[34] Y. Yang, R. Du, C. Shi, J. Zhao, Y. Song, L. Zhang, Z. Ling, Desalination and enrichment of phosphorus-containing wastewater via cyclopentane hydrate, J. Environ. Chem. Eng. 9 (2021) 105507, https://doi.org/10.1016/j.jece.2021.105507.
[35] H.S. Truong-Lam, C. Jeon, J.D. Lee, Thermodynamic and kinetic study of fluorinated gas hydrates for water purification, Can. J. Chem. Eng. 101 (2023) 708–717, https://doi.org/10.1002/cjce.24537.
[36] H. Dong, L. Zhang, Z. Ling, J. Zhao, Y. Song, The controlling factors and ion exclusion mechanism of hydrate-based pollutant removal, ACS Sustain. Chem. Eng. 7 (2019) 7932–7940, https://doi.org/10.1021/acssuschemeng.9b00651.